THE JOURNAL OF BIOLOGICAL CHEMISTRY VOL. 283, NO. 29, pp. 20209–20219, July 18, 2008
© 2008 by The American Society for Biochemistry and Molecular Biology, Inc. Printed in the U.S.A.

A New Branch of Endoplasmic Reticulum Stress Signaling and the Osmotic Signal Converge on Plant-specific Asparagine-rich Proteins to Promote Cell Death*[S]

Received for publication, April 4, 2008, and in revised form, May 2, 2008 Published, JBC Papers in Press, May 19, 2008, DOI 10.1074/jbc.M802654200

Maximiller D. L. Costa[‡1], Pedro A. B. Reis[‡1], Maria Anete S. Valente[‡1], André S. T. Irsigler[‡1,2], Claudine M. Carvalho[‡3], Marcelo E. Loureiro[§], Francisco J. L. Aragão[¶], Rebecca S. Boston[‖], Luciano G. Fietto[‡], and Elizabeth P. B. Fontes[‡4]

From the [‡]Departamento de Bioquímica e Biologia Molecular, BIOAGRO and the [§]Departamento de Biologia Vegetal, Universidade Federal de Viçosa, 36571.000, Viçosa, MG, Brazil, [¶]Embrapa Recursos Genéticos e Biotecnologia, PqEB W5 Norte, 70770-900, Brasília, DF, Brazil, and the [‖]Department of Plant Biology, North Carolina State University, Raleigh, North Carolina 27695

NRPs (N-rich proteins) were identified as targets of a novel adaptive pathway that integrates endoplasmic reticulum (ER) and osmotic stress signals based on coordinate regulation and synergistic up-regulation by tunicamycin and polyethylene glycol treatments. This integrated pathway diverges from the molecular chaperone-inducing branch of the unfolded protein response (UPR) in several ways. While UPR-specific targets were inversely regulated by ER and osmotic stresses, NRPs required both signals for full activation. Furthermore, BiP (binding protein) overexpression in soybean prevented activation of the UPR by ER stress inducers, but did not affect activation of NRPs. We also found that this integrated pathway transduces a PCD signal generated by ER and osmotic stresses that result in the appearance of markers associated with leaf senescence. Overexpression of NRPs in soybean protoplasts induced caspase-3-like activity and promoted extensive DNA fragmentation. Furthermore, transient expression of NRPs *in planta* caused leaf yellowing, chlorophyll loss, malondialdehyde production, ethylene evolution, and induction of the senescence marker gene *CP1*. This phenotype was alleviated by the cytokinin zeatin, a potent senescence inhibitor. Collectively, these results indicate that ER stress induces leaf senescence through activation of plant-specific NRPs via a novel branch of the ER stress response.

The unfolded protein response (UPR)[5] is activated by stress conditions that disrupt the endoplasmic reticulum (ER) homeostasis and the proper folding and maturation of secretory proteins. This complex signaling cascade is conserved in eukaryotes, although the mechanism of signal transduction differs across species. The central transducer of the UPR is IRE1, a transmembrane kinase that appears to be the only means of signal transduction in yeast, but is part of a tripartite signaling response in animals, which also includes the ER-transmembrane transducers PERK and ATF6 (1). In plants, there is compelling evidence that the UPR operates through IRE1 (2–7), but characterization of this cytoprotective signaling pathway is still incipient. The only known components of plant UPR are the putative proximal sensors that include two *Arabidopsis* Ire1p homologues and two ATF6-related proteins, designated AtbZIP28 and AtbZIP60 (8–10). Although the N-terminal domain of plant IRE1 homologues can replace functionally the yeast IRE1, downstream components of the IRE1 signaling are yet to be identified (8). *AtbZIP60* and *AtbZIP28* have been described as ER stress-induced leucine zipper (bZIP) transcription factor genes that are anchored to the ER membrane under normal conditions and may serve as ER stress sensors and transducers (9, 10). Upon sensing the ER stress, AtbZIP28 is proteolytically released from the membrane and translocated to the nucleus by a mechanism that is predicted to be similar to that acting on mammalian ATF6 transducer (10). Expression of a truncated form of either AtbZIP28 or AtbZIP60, harboring the bZIP domain, up-regulates UPR target genes under normal conditions (9, 10).

The UPR up-regulated chaperone BiP (binding protein) is central to this cytoprotective response as the indirect sensor of alterations in the ER environment. In addition to this role as molecular chaperone, in mammalian cells, BiP has been shown to regulate the UPR by controlling the activation status of the three transducers, IRE1, PERK, and ATF6 (11). Under normal conditions, the luminal domains of these sensors are occupied with BiP, which is recruited by unfolded proteins upon ER stress. The dissociation of BiP promotes oligomerization and

* This work was supported in part by the Brazilian Government Agency CNPq Grants 50.6119/2004-1 and 470878/2006-1 (to E. P. B. F.), FAPEMIG Grant EDT 523/07, and FINEP Grant 01.07.610.00 (to E. P. B. F.). The costs of publication of this article were defrayed in part by the payment of page charges. This article must therefore be hereby marked "*advertisement*" in accordance with 18 U.S.C. Section 1734 solely to indicate this fact.

[S] The on-line version of this article (available at http://www.jbc.org) contains supplemental Figs. S1–S6 and Table S1.

[1] Supported by a graduate fellowship from CNPq.

[2] Present address: Molecular Core Facility, Dept. of Biology, Florida State University, Tallahassee, FL 32306-4370.

[3] A FAPEMIG (CBB 00112/07) postdoctoral fellow.

[4] To whom correspondence should be addressed: Departamento de Bioquímica e Biologia Molecular/BIOAGRO, Universidade Federal de Viçosa, 36571.000 Viçosa, MG, Brazil. Tel.: 55-31-3899-2949; Fax: 55-31-3899-2864; E-mail: bbfontes@ufv.br.

[5] The abbreviations used are: UPR, unfolded protein response; AZC, L-azetidine-2-carboxylic acid; BAP, 6-benzylaminopurine; BiP, binding protein; CNX, calnexin; CRT, calreticulin; DCD, development and cell death; ER, endoplasmic reticulum; MDA, malondialdehyde; NIG, NSP-interacting GTPase; NRPs, N-rich proteins; PCD, programmed cell death; PDI, protein-disulfide isomerase; PEG, polyethylene glycol; SMP, seed maturation protein; MES, 4-morpholineethanesulfonic acid; GFP, green fluorescent protein; TUNEL, terminal deoxynucleotidyltransferase-mediated dUTP nick end-labeling; WT, wild type; RACE, rapid amplification of cDNA ends.

Downloaded from http://www.jbc.org/ at CAPES - EMBRAPA on May 21, 2018

phosphorylation of IRE1 and PERK, as well as relocalization of ATF6 to the Golgi where its transcriptional domain is proteolytically released from the membrane into the nucleus. Although the UPR has not been extensively characterized in plants, conserved aspects between mammalian and plant UPR include its negative regulation by BiP, possibly through interaction with the putative proximal sensors, and the BiP cytoprotective role (12). In fact, we have previously demonstrated that BiP confers tolerance to water deficit in transgenic plants (13).

Constant challenges by adverse conditions and environmental stresses pose major constraints for development, growth, and productivity of plants. Our knowledge about stress-specific adaptive responses and cross-talk between signaling cascades has advanced considerably with genome-wide analyses and expression-profiling studies in different plant species under different stress conditions (14–16). A common theme that has emerged is that plants transduce environmental signals through integrated networks between different stress-induced adaptive responses. Despite the potential of ER stress response to accommodate adaptive pathways, its integration with environmental-induced responses is poorly understood in plants. Recently, we performed global expression profiling on soybean leaves exposed to polyethylene glycol (PEG) treatment or to UPR inducers to identify integrated networks between osmotic and ER stress-induced adaptive responses (4). In addition to uncovering specific responses to ER stress and osmotically regulated changes, a small proportion (5.5%) of the up-regulated genes represented a shared response that seemed to integrate the two signaling pathways. These co-regulated genes had similar induction kinetics and a synergistic response to the combination of osmotic- and ER stress-inducing treatments. Thus, they were considered to be downstream targets of the integrating pathway. Two ESTs (N-richI and N-richII), which showed the strongest synergistic induction, were homologous to genes encoding asparagine-rich proteins that have a plant-specific development and cell death (DCD) domain. Here we investigated the possibility that the integrated pathway might transduce a programmed cell death (PCD) signal generated by ER and osmotic stress. We demonstrated that induction of target genes, such as N-richI and N-richII ESTs, by ER stress-inducing agents occurs via a pathway distinct from the UPR. We also found that the N-rich proteins are critical mediators of osmotic- and ER stress-induced cell death in plants.

EXPERIMENTAL PROCEDURES

Plant Growth, Soybean Suspension Cells, and Stress Treatments—Soybean (*Glycine max*) seeds (cultivar Conquista) were germinated in soil and grown under greenhouse conditions (avg: 21 °C, max: 31 °C, min: 15 °C) under natural conditions of light, 70% relative humidity, and approximately equal day and night length. Two weeks after germination, the seedlings were transferred to a 2-ml 10 μg/ml tunicamycin (Sigma) solution (DMSO, as control). After 12 and 24 h of treatment, the leaves were harvested, immediately frozen in liquid N_2, and stored at −80 °C until use.

Alternatively, the aerial portions of 3-week-old plants were excised below the cotyledons and directly placed into 15 ml of 10% (w/v) polyethylene glycol (PEG; MW 8000, Sigma), 10 μg/ml tunicamycin (Sigma), or 50 mM L-azetidine-2-carboxylic acid (AZC, Sigma) solutions. The first trifoliate leaves were harvested after 4, 10, or 16 h of PEG and tunicamycin treatments, then immediately frozen in liquid N_2, and stored at −80 °C until use. Each stress treatment and RNA extraction were replicated in three independent experiments.

Cotyledons cells from the soybean variety Conquista were cultured as described previously (17). Cells were subcultured every 10 days by diluting the culture 1:10 in fresh MS medium. All treatments were performed on 5-day-old subcultures. Tunicamycin was added to cultures by dilution of a 5 mg/ml stock in DMSO into normal growth medium to 10 μg/ml and incubated for the intervals indicated in the figure legends. For PEG-induced dehydration, the cells were washed and then cultured with normal growth medium containing 10% (w/v) PEG-8000 for the indicated intervals. Suspension cells were directly treated with 0.5 μg/ml cycloheximide, 10 μM BAP (6-benzylaminopurine), and 10 μM zeatin for the intervals indicated in the figure legends. After treatments, the cells were filtrated under vacuum, washed with 0.25 M NaCl, and immediately frozen in liquid N_2.

Rapid Amplification of 3′-cDNA Ends (3′-RACE) and NRP-B cDNA Cloning—3′-RACE was performed using the GeneRacer kit (Invitrogen). Total RNA isolated from PEG-treated soybean leaves was used for reverse transcription, and an N-richI EST-specific primer (FwNRich1, TACAGGCATCCAATTTGGCGAACC) and oligo dT primer from the kit were used in the polymerase chain reaction. The amplified fragment was cloned in pCR4 to generate pCR4-NRPB, which harbors the full-length NRP-B cDNA.

Plasmid Construction—For transient expression in protoplasts, NRP-B and NRP-A (gi:57898928) cDNAs were amplified and inserted into the BglII and EcoRI sites of pMON921 (18). The resulting clones pUFV967 and pUFV849 contain NRP-B or NRP-A cDNAs, respectively, under the control of the cauliflower mosaic virus 35S promoter and the 3′-end of the pea E9 *rbcS* gene. For agroinfiltration in tobacco leaves, NRP-A and NRP-B cDNAs were amplified by PCR and introduced by recombination into the entry vector pCR8/GW/TOPO (Invitrogen) to generate pUFV908 and pUFV874, respectively. NRP-A and NRP-B cDNAs were then transferred by recombination to the plant transformation binary vector 35S-YFP-cassetteA-Nos-pCAMBIA1300 yielding pUFV937 (35S:NRP-B) and pUFV938 (35S:NRP-A), which contain NRP-B or NRP-A cDNA, respectively, under the control of the 35S promoter and 3′-ends of *nos*. For subcellular localization, NRP-A and NRP-B cDNAs were amplified by PCR with appropriate extensions and introduced by recombination into the entry vector pDONR201 (Invitrogen) and then transferred to the binary vector pK7FWG2 to generate pK7F-NRP-B and pK7F-NRP-A, which contain the *GFP* gene fused in-frame after the last codon of the respective cDNAs. The U16322 plasmid harboring a full-length *NIG* (NSP-interacting GTPase, Ref. 19). cDNA was obtained from the *Arabidopsis* Biological Resource Center (ABRC) and used as a control. For this purpose, the full-length *NIG* cDNA was amplified by PCR from U16322 cDNA, cloned into pDONR201 and then transferred to the binary vector pK7WG2

Downloaded from http://www.jbc.org/ at CAPES - EMBRAPA on May 21, 2018

to obtain pK7-NIG, which contains NIG cDNA under the control of the CaMV 35S promoter.

Real-time RT-PCR Analysis—For quantitative RT-PCR, total RNA was extracted from frozen leaves or cells with TRIzol (Invitrogen) according to the instructions from the manufacturer. The RNA was treated with 2 units of RNase-free DNase (Promega) and further purified through RNeasy Mini kit (Qiagen) columns. First-strand cDNA was synthesized from 4 μg of total RNA using oligo-dT(18) and Transcriptase Reversa M-MLV (Invitrogen), according to the manufacturer's instructions.

Real-time RT-PCR reactions were performed on an ABI7500 instrument (Applied Biosystems), using SYBR® Green PCR Master Mix (Applied Biosystems). The amplification reactions were performed as follows: 2 min at 50 °C, 10 min at 95 °C, and 40 cycles of 94 °C for 15 s and 60 °C for 1 min. To confirm quality and primer specificity, we verified the size of amplification products after electrophoresis through a 1.5% agarose gel, and analyzed the T_m (melting temperature) of amplification products in a dissociation curve, performed by the ABI7500 instrument. The primers used are listed in supplemental Table S1. For quantitation of gene expression in soybean protoplasts and seedlings, we used RNA helicase (4) as the endogenous control gene for data normalization in real-time RT-PCR analysis. For quantitation of gene expression in tobacco leaves, we used actin as a control gene.

Fold variation, which is based on the comparison of the target gene expression (normalized to the endogenous control) between experimental and control samples, was quantified using the comparative Ct method: $2^{-}(\Delta Ct_{Treatment} - \Delta Ct_{Control})$. The absolute gene expression was quantified using the 2-ΔCT method, and values were normalized to the endogenous control.

Soybean Transformation—A plant expression cassette containing the *BiPD* gene was constructed by insertion of the 2.0-kb XbaI cDNA insert of pUFV24 (17) into the pBS35SdAMVNOS2 vector. The resulting clone pBS35SdAMVNOS2-BiP contains the BiP cDNA under control of a duplicated cauliflower mosaic virus 35S promoter with an enhancer region from the alfalfa mosaic virus and the polyadenylation signal of the *nos* gene. The *Arabidopsis thaliana ahas* gene (that confers tolerance to the herbicide imazapyr) was removed from the vector pAC321 (20) with XbaI and inserted into the vector pFACM1 to generate pFACMahas. The *BiPD* expression cassette was released with SalI and NotI from pBS35SdAMVNOS2-BiP and cloned into the vector pFACMahasm to yield pahasBip. The vector pahasBip was used to transform soybean (cv. Conquista) as previously described (20). Primary transformants were selected by PCR using the primers bipsoy235 (5′-GAGAGACTAATTGGAGAGGCTG-3′) and bipsoy645c (5′-ATAGGCAATGGCAGCAGCAGTG-3′), which amplify a 410-bp sequence from the *BiPD* gene coding region and cover an intron region from the genomic BiPD sequence. Segregation analyses of independently transformed soybean lines were performed by PCR, and accumulation of BiP was monitored in each subsequent generation by immunoblotting.

RNA Gel Blotting—Total RNA was extracted from frozen leaves of control and tunicamycin-treated wild type and soybean transgenic seedlings, which were treated with tunicamycin or control DMSO for 24 h, with TRIzol (Invitrogen) according to the instructions from the manufacturer. Equal amounts of total RNA were denatured by formamide/formaldehyde and resolved on 1% agarose gels containing formaldehyde. The RNA was transferred to a nylon membrane by capillary transfer and immobilized by UV cross-linking (Stratalinker, Stratagene). The membrane was hybridized at high stringency conditions using the soyBiPD cDNA (17) as probe. The hybridization probe was radiolabeled with [α-^{32}P]dCTP by random primed labeling (Amersham Biosciences). Autoradiography was performed at −80 °C using a Lightning-Plus intensifying screen. The amount of RNA and the integrity of ribosomal RNA were monitored by rehybridizing the membranes with an 18 S rDNA probe.

Immunoblot Analysis—Total protein was extracted from control and tunicamycin-treated leaves of wild-type and soybean transgenic seedlings as previously described (17). SDS-PAGE was carried out, and the proteins were transferred from 10% SDS-polyacrylamide gels to nitrocellulose membranes by electroblotting. Immunoblot analyses were performed using polyclonal anti-BiP-carboxyl antibodies (2), an anti-calreticulin serum (21) or an anti-GmSBP2 serum (22) at a 1:1000 dilution and a goat anti-rabbit IgG alkaline phosphatase conjugate (Sigma) at a 1:5000 dilution. Alkaline phosphatase activity was assayed using 5-bromo-4-chloro-3-indolyl phosphate (Sigma) and *p*-nitro blue tetrazolium (Sigma).

Transient Expression in Soybean Protoplasts—Protoplasts were prepared from soybean suspension cells as essentially described by Fontes *et al.* (18). The protoplasts were isolated 5 days after subculture by digestion for 3 h, under agitation at 40 rpm, with 0.5% cellulase, 0,5% macerozyme R-10, 0.1% pectolyase Y23, 0.6 M mannitol, 20 mM MES, pH 5.5. The extent of digestion was monitored by examining the cells microscopically at each 30-min interval. After filtration through nylon mesh of 65 μm, protoplasts were recovered by centrifugation, resuspended in 2 ml of 0.6 M mannitol, 20 mM MES, pH 5.5, separated by centrifugation in a sucrose gradient (20% (w/v) sucrose, 0.6 M mannitol, 20 mM MES, pH 5.5), and diluted into 2 ml of electroporation buffer (25 mM Hepes-KOH, pH 7.2, 10 mM KCl, 15 mM $MgCl_2$, 0.6 M mannitol). Transient expression assays were performed by electroporation (250 V, 250 μF) of 10 μg of expression cassette DNA, and 30 μg of sheared salmon sperm DNA into $2 \times 10^5 - 5 \times 10^6$ protoplasts in a final volume of 0.8 ml. Protoplasts were diluted into 8 ml of MS medium supplemented with 0.2 mg/ml 2,4-dichlorophenoxyacetic acid and 0.6 M mannitol, pH 5.5. After 36 h of incubation in the dark, the protoplasts were washed with 0.6 M mannitol, 20 mM MES, pH 5.5, and frozen in liquid N_2 until use.

Caspase-3-like Activity and in Situ Labeling of DNA Fragmentation (TUNEL)—Total protein was extracted from soybean cells 36-h post-electroporation. Caspase-3-like activity was determined using the ApoAlert® Caspase-3 Colorimetric Assay kit (Clontech) according to the manufacturer's instructions. The substrate was DEVD-pNA, and the inhibitor of caspase-3 activity was the synthetic tetrapeptide DEVD-fmk

Downloaded from http://www.jbc.org/ at CAPES - EMBRAPA on May 21, 2018

supplied by the kit. Free 3′-OH in the DNA was labeled by the terminal deoxynucleotidyl transferase-mediated dUTP nick-end labeling (TUNEL) assay using the ApoAlert DNA Fragmentation Assay kit (Clontech) as instructed by the manufacturer. Samples were observed with a Zeiss LSM 410 inverted confocal laser scanning microscope fitted with the configuration: excitation at 488 nm and emission at 515 nm. As a positive control, samples were treated with DNase1.

Transient Overexpression in Nicotiana tabacum by Agrobacterium Infiltration—*N. tabacum* plants were grown in a greenhouse with natural day length illumination. Three weeks after germination, the plants were transferred to a growth chamber at 21 °C with a 16-hour light and 8-hour dark cycle. Agrobacterium infiltration was performed in the leaves of *N. tabacum* with *Agrobacterium* strain GV3101 carrying pUFV937 (35S:NRP-B) or pUFV938 (35S:NRP-A), NIG (35S:NIG), rpl10 (35S:rpL10) as previously described (23).

Subcellular Localization of Proteins—For subcellular localization of proteins, *N. tabacun* leaves were agroinoculated with pK7F-NRP-B and pK7F-NRP-A. About 72-h post-agroinfiltration, 1-cm^2 leaf explants were excised incubated with 0.6 M mannitol for 10 min, and GFP fluorescence patterns were examined in epidermal cells with ×40 oil immersion objective and a Zeiss LSM510 META inverted laser scanning microscope equipped with an argon laser as excitation source. For imaging GFP, the 455-nm excitation line and the 500–530-nm band pass filter were used. The pinhole was usually set to give a 1–1.5-μm optical slice. Post-acquisition image processing was done using the LSM 5 Browser software (Carl-Zeiss) and Adobe Photoshop (Adobe Systems). Microsomal fractions were prepared from agroinoculated leaves, as described (24), and immunoblotted with an anti-GFP serum.

Determination of Chlorophyll Content and Lipid Peroxidation—Total chlorophyll content was determined spectrophotometrically at 663 and 646 nm after quantitative extraction from individual leaves with 80% (v/v) acetone in the presence of ~1 mg of Na_2CO_3 (25). The extent of lipid peroxidation in leaves was estimated by measuring the amount of MDA (malondialdehyde, a decomposition product of the oxidation of polyunsaturated fatty acids). MDA content was determined by the reaction of thiobarbituric acid (TBA) as described by Cakmak and Horst (26).

Ethylene Determination—For ethylene measurements as a function of NRP-A and NRP-B expression, whole leaves of 3-week-old tobacco plants were agroinoculated with pK7-NRP-A, pK7-NRP-B, or control binary vector. Agroinfiltrated tobacco plants were placed in 25-ml flasks containing a Petri dish with 3 ml of 1 M $HgClO_4 \cdot 4H_2O$ and sealed with rubber serum caps. After 5 days, the solution was collected into a sealed assay tube, and ethylene was released with the injection of 1 ml of 1 M KCl. 1 ml of gas was collected with a syringe, and ethylene was measured on a model 5840A gas chromatography system (Hewlett-Packard Canada Ltda) equipped with a flame ionization detector. A Porapak N (80–100 mesh, 100 cm × 6 mm) column was used at 60 °C. The injection port and detector temperatures were 100 and 150 °C, respectively. The flow of nitrogen, air, and hydrogen was at 30, 130, and 20 ml min^{-1}, respectively.

RESULTS

N-richI and N-richII ESTs Are Both Encoded by the NRP-B Gene—The N-richI and N-richII ESTs correspond to different regions of a contiguous soybean genomic sequence (scaffold_78:2951370.2949024). To determine if both ESTs corresponded to the same mRNAs, we obtained the full sequences of N-richI and N-richII cDNAs through RACE. A comparison of the cDNA sequences revealed that these ESTs represented the same gene which we designated *NRP-B* (N-rich protein B; supplemental Fig. S1*A*). The deduced NRP-B protein has an estimated M_r of 37092 and pI 7.05 and is most closely related to the previously identified NRP from soybean (27), here designated NRP-A. The two NRPs share a highly conserved C-terminal DCD domain in addition to a high content of asparagine residues at their more divergent N termini. This structural organization places NRP-A and NRP-B in the subgroup I of plant-specific DCD-containing proteins (28). Analysis of several subgroup I DCD domain-containing proteins by ClustalW showed that NRP-A and NRP-B form a subgroup with the *Arabidopsis* protein of unknown function encoded by At5g42050 (gi 231 18422167, supplemental Fig. S1*B*). An examination of available microarray data indicated that the At5g42050 locus is induced by cycloheximide, osmotic stress, salt stress, and during senescence (GeneInvestigator).

Integration of ER Stress and Osmotic Signals Leads to Maximal Expression of NRP-A—The high degree of sequence similarity between NRP-B and NRP-A prompted us to ask whether NRP-A was also a target of the ER and osmotic stress integrating pathway. Expression analysis was carried out by quantitative RT-PCR (Fig. 1). Like *NRP-B*, *NRP-A* is up-regulated by the ER stress inducers AZC, dithiothreitol, or tunicamycin that cause protein misfolding in the ER by different mechanisms (supplemental Fig. S2). The L-proline analogue AZC is incorporated into proteins competitively with L-proline, tunicamycin inhibits Asn-linked glycosylation, and dithiothreitol prevents disulfide bond formation. Very likely, induction of *NRP-A* and *NRP-B* by these chemicals is a result of accumulation of misfolded proteins in the ER rather than a result of a specific protein dysfunction unrelated to ER stress.

Osmotic and ER stress each promoted rapid induction of *NRP-A* expression that showed a kinetic pattern similar to that observed for *NRP-B* induction (Fig. 1*A*). When combined, AZC and PEG treatments promoted a synergistic effect on accumulation of both *NRP-A* and *NRP-B* transcripts (Fig. 1*B*). Based on these criteria, we concluded that *NRP-A*, like *NRP-B,* was a target of the previously described ER and osmotic stress integrating pathway, which we will refer to here as the integrated pathway (4).

Up-regulation of NRP-A and NRP-B by UPR Inducers Occurs through a Novel Signaling Branch of the ER Stress Response—UPR target genes that encode components of the ER protein processing machinery have been shown to exhibit a differential and antagonistic regulation by ER stress inducers and PEG-induced dehydration (4). The UPR genes, such as *BiPD*, *BiPC*, *CNX* (calnexin), and *PDI* (protein-disulfide isomerase), are not only down-regulated by osmotic stress but generally show a progressively enhanced effect with an increase in the duration

Downloaded from http://www.jbc.org/ at CAPES - EMBRAPA on May 21, 2018

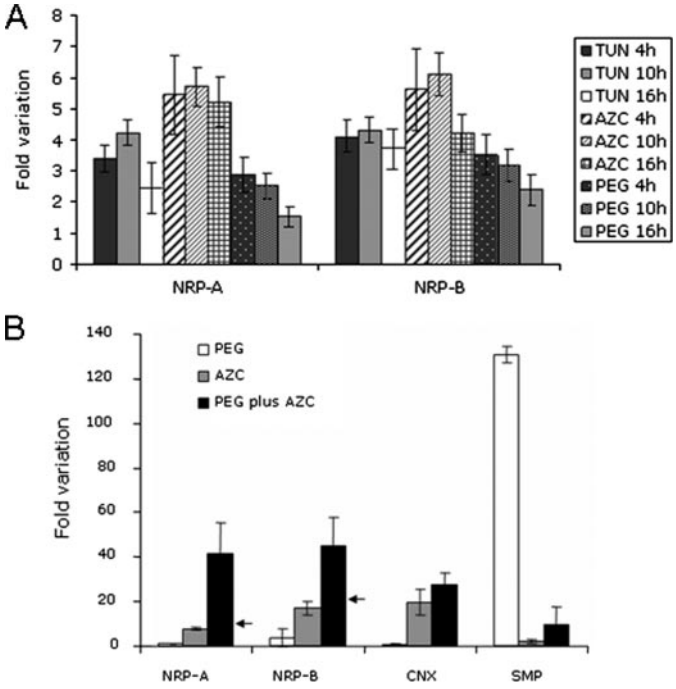

FIGURE 1. **Osmotic and ER stress determine full expression of soybean *NRP-A* and *NRP-B* genes.** *A*, time course of *NRPs* induction by PEG, tunicamycin, and AZC treatments in soybean seedlings. Plants were treated with tunicamycin (*TUN*), AZC, or PEG for the indicated period of time. The fold variation of gene expression was determined by real-time RT-PCR. Values are relative to H_2O or DMSO control treatments (±S.D., $n = 3$ biological replicates). *B*, *NRP-A* and *NRP-B* are synergistically induced when treated with both PEG and AZC, as determined by quantitative PCR. Soybean plants were treated for 16 h with PEG, AZC, or a combination of AZC and PEG. *CNX* indicates calnexin transcripts, and *SMP* refers to a seed maturation protein transcripts used as specifically tunicamycin- or PEG-induced control genes, respectively. Values are relative to H_2O control treatment for 16 h (± S.D., $n = 3$ biological replicates). *Arrows* indicate the level of additive responses.

of the PEG treatment (supplemental Fig. S3). In contrast, up-regulation of the integrated pathway, represented by the target *NRP-A* and *NRP-B* genes, showed a persistent pattern throughout prolonged PEG and tunicamycin treatments. These results suggest that the integrated pathway genes and the UPR-specific genes may be regulated by osmotic stress via independent pathways. In addition, they raise the question as to whether the integrated pathway shares components with the UPR pathway or is a separate, parallel pathway. To address this issue we examined *NRP-A* and *NRP-B* induction under conditions that prevent activation of UPR. Because plant UPR has not been fully characterized and therefore loss-of-function mutants are lacking in the plant kingdom, we proceeded to obtain gain-of-function transgenic lines that had a dampened UPR.

In both mammals and plants, *BiP* overexpression has been shown to inhibit activation of UPR (11, 12). We used a similar strategy and obtained soybean transgenic lines ectopically expressing the soyBiPD cDNA under the control of the 35S promoter. These independently transformed overexpression (OE) lines constitutively accumulated higher levels of BiPD mRNA (Fig. 2*A*) and protein (Fig. 2*B*) than untransformed wild-type controls. To examine the capacity of the OE lines to induce a UPR, we treated seedlings from the highest OE line with tunicamycin and assayed for expression of *BiP* and also calreticulin (*CRT*), which we used as a UPR response gene. The 35S-BiP-4 transgenic line expressed BiP mRNA at levels similar to the untransformed wild-type line after tunicamycin treatment and displayed only marginal variations in the level of BiP mRNA after ER stress-inducing treatments (Fig. 2*C*). The OE line showed a slight increase in the levels of BiP mRNA after 12 h of tunicamycin treatment and had slightly less BiP mRNA by 24 h of treatment. We also analyzed protein levels, and we found that the BiP-overexpressing line continued to have slightly higher levels of BiP than those observed in the wild-type line after UPR induction (Fig. 2*D*). As expected, however, induction of calreticulin was seen only in the WT plants; the BiP-overexpressing line (35S-BiP) lacked the capacity to induce calreticulin protein in response to tunicamycin treatment.

Because the Northern probe does not discriminate between the *BiP* transgene and endogenous *BiP* genes, we also analyzed expression with gene-specific primers to quantify only the endogenous soyBiPD mRNA. In the *soyBiPD* transgene construct, the 3′-untranslated sequences are replaced with *nos* 3′ sequences so a primer from the native 3′ would not recognize the transgene (29). The homozygous soybean 35S-BiP-4 transgenic line was treated with tunicamycin and the induction of UPR was evaluated by quantifying transcript accumulation of typical UPR-specific targets (*BiP* and *CNX*) by real-time RT-PCR (Fig. 2*E*). Our results confirmed that overexpression of soy*BiPD* in soybean transgenic lines attenuated UPR activation as revealed by decreased induction of the endogenous BiP (*BiPD*) and *CNX* genes under conditions that promote ER stress in the wild-type controls (Fig. 2*E*). In contrast, inhibition of UPR activation by BiP did not alter the induction profile of *NRP-A* and *NRP-B* genes by tunicamycin. In addition, overexpression of *NRP-A* and *NRP-B* in soybean protoplasts did not up-regulate UPR targets, such as *BiP* and *CNX* (Fig. 2*F*). These results strongly indicate that induction of *NRP-A* and *NRP-B* genes by ER stress inducers occurs through a different signaling branch of the ER stress response than the ER chaperone-inducing UPR branch.

This integrated pathway diverged further from characterized ER-specific branches of UPR as downstream targets were inversely regulated by osmotic stress in untransformed soybean plants (supplemental Fig. S3 and Ref. 4). In addition, the integrated pathway genes *NRP-A* and *NRP-B* exhibited a strong synergistic response to the combination of osmotic and ER stress-inducing treatments (Fig. 1*B*). Collectively, our results describe a novel branch of the ER stress response that integrates the osmotic signal to potentiate transcription of shared target genes, such as *NRP-A* and *NRP-B*.

NRP-A and NRP-B Induce Apoptotic-like Cell Death in Soybean Suspension Cells—NRP-A and *NRP-B* encode a DCD domain that has been suggested to be involved in the hypersensitive response and programmed cell death (25, 26). If so, we predicted that they would be involved in transducing a PCD signal through the integrated pathway. To examine whether these genes are involved in cell death, we assayed several different aspects of PCD: acute induction of PCD by cycloheximide, activation of caspase-like activities, DNA fragmentation, inhibition of the developmental PCD pathway associated with senescence, and induction of senescence markers by overexpression of *NRP-A* and *NRP-B*.

Downloaded from http://www.jbc.org/ at CAPES - EMBRAPA on May 21, 2018

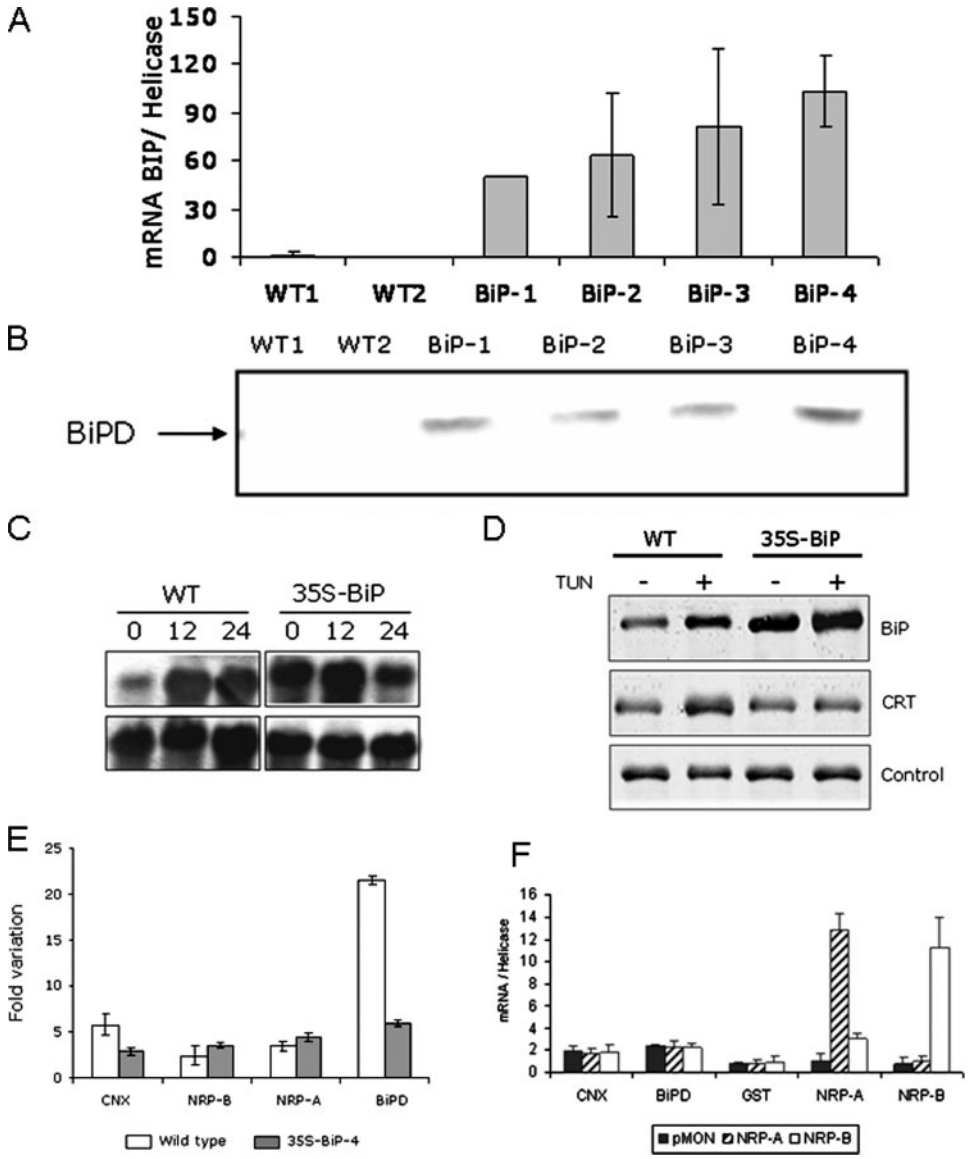

FIGURE 2. **A defective UPR in BiP-overexpressing soybean lines does alter induction of *NRP* genes by tunicamycin.** *A*, transcript accumulation of *soyBiPD* transgene in soybean transgenic lines under normal conditions. Total RNA was isolated from leaves of untransformed wild-type (*WT1* and *WT2*) plants and independently transformed soybean lines (35S-BiP-1, 35S-BiP-2, 35S-BiP-3, and 35S-BiP-4) and *BiP* transgene transcript levels were quantified by real-time PCR, using transgene-specific primers. Values represent the mean ± S.D. of three replicates. *B*, enhanced levels of BiP in soybean transgenic lines. Equal amounts of total proteins (30 μg) from the indicated lines were immunoblotted with anti-BiP-carboxyl antibodies. *C*, UPR induction by treatment of soybean seedlings with tunicamycin. Soybean seedlings of wild type (*WT*) and homozygous 35S-BiP-4 (35*S-BiP*) lines were treated with tunicamycin for 0, 12, or 24 h, and *BiP* expression was monitored by Northern blotting with soyBiPD cDNA as probe. *Bottom*, the membrane was reprobed with an 18 S rDNA probe. *D*, accumulation of UPR-specific proteins in response to tunicamycin treatment. Equivalent amounts of total protein (40 μg) extracted from untreated (−) and tunicamycin-treated (+) WT or 35S-BiP-4 (35*S-BiP*) seedlings were immunoblotted with an anti-BiP-carboxyl (*BiP*), calreticulin (*CRT*) antiserum, or an antibody against a UPR-unrelated protein (*GmSBP2*). *E*, *NRP-A* and *NRP-B* induction by tunicamycin in soybean transgenic lines defective for UPR activation. The fold variation was determined by real-time RT-PCR from wild type and 35S-BiP-4 transgenic seedlings treated with tunicamycin for 16 h. Values are relative to DMSO control treatment for 16 h and represent the mean ± S.D. of three replicates from three independent experiments. *F*, transient overexpression of NRP-A or NRP-B in soybean protoplasts does not affect *BiP* and *CNX* expression. Plasmids containing the *NRP-A* or *NRP-B* expression cassette were electroporated in soybean protoplasts and transient gene expression was monitored by quantitative RT-PCR. pMON indicates electroporation with the empty vector. *GST* is a control gene. Values represent the mean ± S.D. of three replicates from two independent experiments.

Treatment with cycloheximide, a cell death inducer in soybean cultured cells (30), resulted in significant increases in *NRP-A* and *NRP-B* transcript accumulation (Fig. 3*A*). A time course experiment in soybean cultured cells demonstrated that both genes are rapidly induced by cycloheximide as soon as 30 min after treatment (supplemental Fig. S4). The induction kinetics of *NRP-A* and *NRP-B* by cycloheximide was similar to their rapid tunicamycin and PEG induction profile and differed from the delayed tunicamycin-induction kinetics of the UPR-specific target *CNX*, which was not strongly induced by cycloheximide. This result suggests that induction of *NRP-A* and *NRP-B* by the cell death inducer cycloheximide may be connected to the integrated pathway.

To directly assess the involvement of NRP-A and NRP-B in cell death, we monitored the induction of caspase-3-like activity, as a biochemical marker of cells committed to apoptosis. Previous studies in plants have shown that different types of proteolytic enzymes, including caspase-3-like activity, are linked to developmental and pathogen- and stress-induced PCD (31). In addition, caspase-3 has been characterized as a downstream protease in the effector phase of PCD in mammals (32), and recent evidence has demonstrated its possible involvement in plant PCD as well (33). We used transient expression of both *NRP-B* and *NRP-A* in soybean protoplasts under the control of the 35S promoter (Fig. 3*B*) as our experimental system. Expression is shown relative to a helicase marker to control for any variation in transformation efficiency. Analysis of caspase-3-like activity (Fig. 3*C*), in protein extracts from *NRP-A*- and *NRP-B*-overexpressing cells revealed a 2.6- and 2.3-fold increase in caspase-3-like activity, respectively, as compared with control, pMON921-transformed protoplasts. Inclusion of a caspase-3-specific inhibitor (DEVD-fmk) reduced enzyme activity to basal levels.

To confirm that the increase in caspase-3-like activity was associated with PCD in the soybean protoplasts, we employed the terminal TUNEL technique to measure fragmentation of DNA in individual cells 36-h postelectroporation. A distinct feature of PCD is the extensive cleavage of nuclear DNA into oligonu-

Downloaded from http://www.jbc.org/ at CAPES - EMBRAPA on May 21, 2018

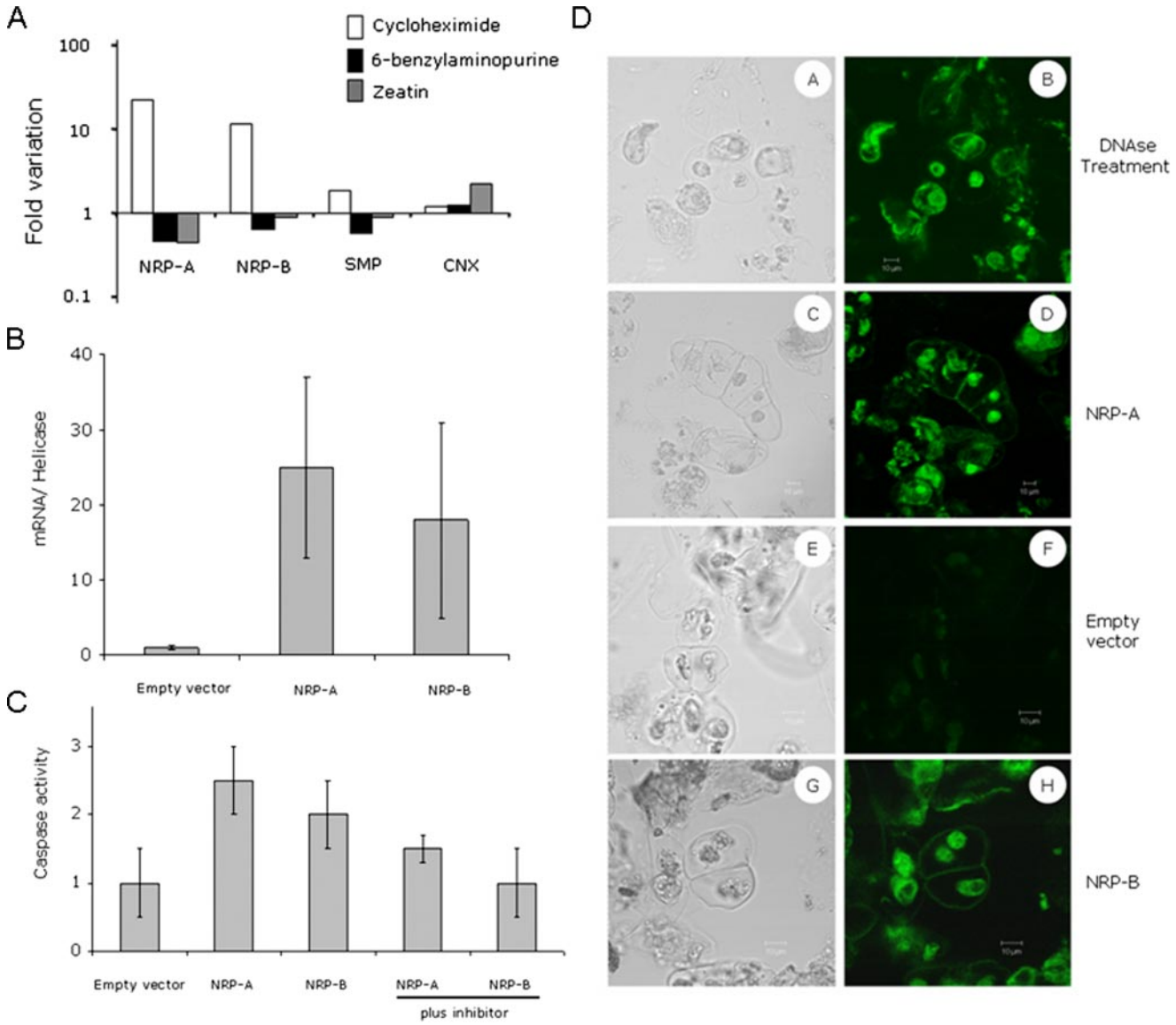

FIGURE 3. **NRP-A and NRP-B induce programmed cell death in soybean protoplasts.** *A*, regulation of *NRP-A* and *NRP-B* by cell death inducers and inhibitors. Treatments, as indicated, were applied on 5-day-old subcultures of soybean suspension cells for 2 h. RNA was isolated and quantified by real-time RT-PCR. Values are relative to control treatment and represent the mean ± S.D. of three replicates from three independent experiments. *B*, transient expression of *NRP-A* and *NRP-B* in soybean protoplasts. Plasmids containing *NRP-A* or *NRP-B* expression cassettes were electroporated in soybean protoplasts, and transient gene expression was monitored by quantitative RT-PCR. *C*, caspase-3-like activities as a function of *NRP-A* and *NRP-B* expression. Total protein was extracted from *NRP-A* and *NRP-B* electroporated protoplast 36 h after, and caspase-3-like activities were monitored with DEVD-pNA substrate in the absence and presence of a specific inhibitor. Values represent the mean ± S.D. of three replicates. *D*, DNA fragmentation promoted by *NRP-A* and *NRP-B* expression. Cells were sampled 36-h postelectroporation of soybean protoplasts with empty vector, *NRP-A* or *NRP-B* expression cassettes, and submitted to TUNEL labeling. As a positive control, untransfected cells were also treated with DNase. Bright fields show the semi-protoplasted cells used in the experiment that confirmed the stained nuclei.

cleosome-sized fragments, which can be detected by the incorporation of fluorescein 12-dUTP at free 3′-OH ends in DNA from the samples. The results of the TUNEL assay are shown in Fig. 3*D*. Control cells transformed with the empty vector exhibited mostly TUNEL-negative nuclei (*panel F*) with only a background level of staining, whereas *NRP-A*- and *NRP-B*-expressing protoplasts had TUNEL-positive nuclei that showed the same extent of staining as DNase-treated positive controls (compare in Fig. 3*D*, *panels B–H*). These results suggest that NRP-A and NRP-B promote apoptotic-like cell death when transiently expressed in protoplasts.

NRP-A and NRP-B Induce Senescence in Planta—To further investigate the role of NRP-A and NRP-B in cell death, we assayed for hallmarks of senescence after manipulating levels of cytokinins. The cytokinins BAP (6-benzylaminopurine) and zeatin have been shown to be potent inhibitors of senescence (34). In a soybean cell cultures, both BAP and zeatin strongly repressed *NRP-A* expression and slightly down-regulated *NRP-B* (Fig. 3*A*). To examine the role of NRP-A and NRP-B *in planta,* we performed gain-of-function experiments by transiently expressing the *NRP* genes in tobacco leaves. The corresponding cDNAs were transferred to binary vectors for Agrobacterium-mediated plant transformation, and the transient expression of the respective genes was induced by agroinoculation into tobacco leaves (Fig. 4). After 1 week, the leaf sectors that were agroinfiltrated with the DNA constructs

Downloaded from http://www.jbc.org/ at CAPES - EMBRAPA on May 21, 2018

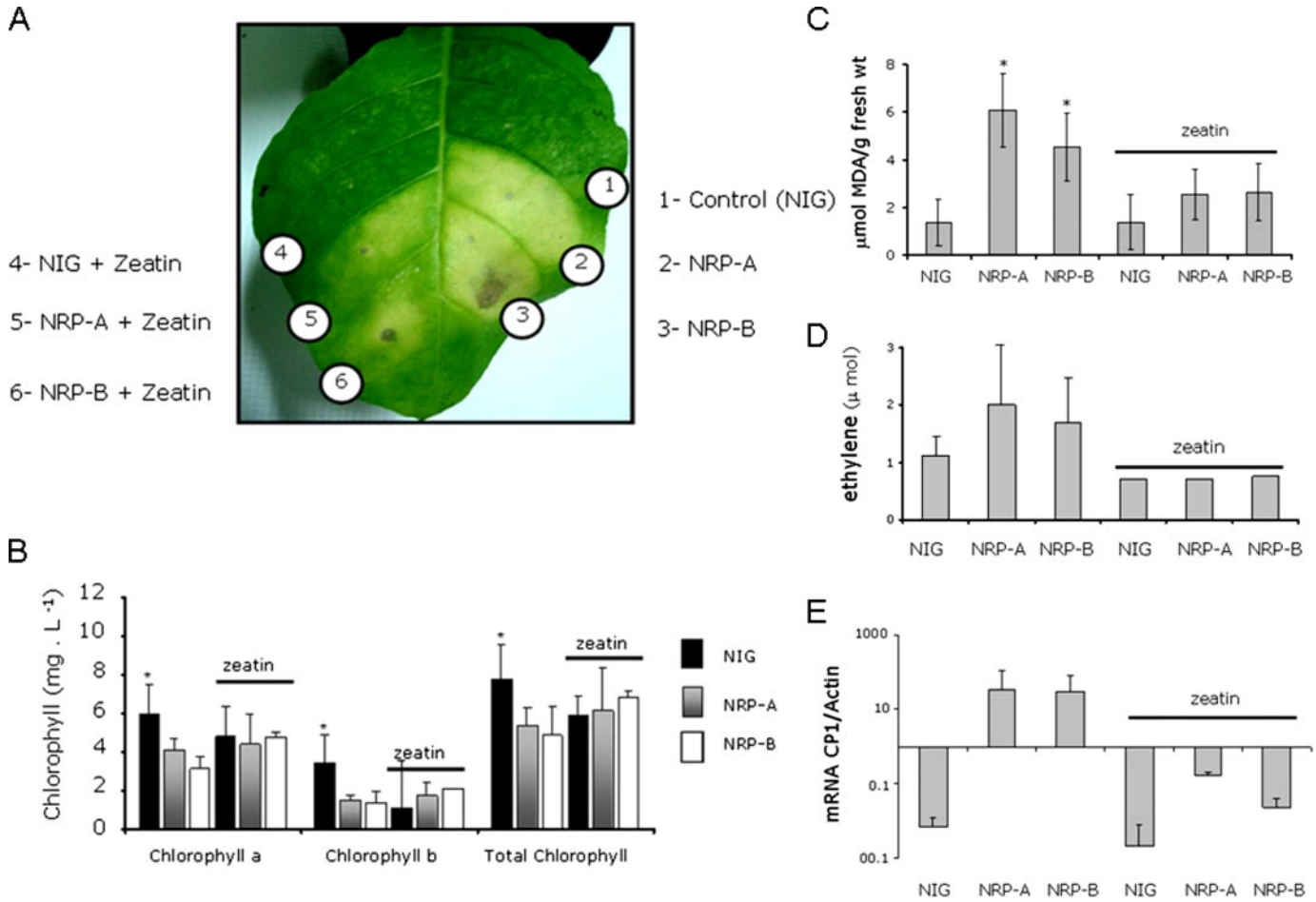

FIGURE 4. **NRP-A and NRP-B promote leaf senescence *in planta*.** 3-week-old plants were infiltrated with agrobacterium cells transformed with p35S:NRP-A and p35S:NRP-B expression vectors or with control binary expression vectors harboring the unrelated *NIG* (p35S:NIG) gene from *Arabidopsis*. In parallel experiments, agroinoculum counterparts were supplemented with the senescence inhibitor zeatin. *A*, yellowing symptoms caused by *NRP-A* and *NRP-B* expression. Leaf sectors were agroinfiltrated with the indicated agroinoculum, and pictures were taken 6 days after infiltration. *B*, chlorophyll loss induced by *NRP-A* and *NRP-B* expression. Total chlorophyll, chlorophyll *a* and *b* were determined from the leaf sectors agroinfiltrated with the indicated samples as in *A*. Values are given as mean ± S.D. from three replicates. *Asterisks* indicate values significantly different ($p < 0.05$, Student's *t* test). *C*, lipid peroxidation in p35S:NRP-A- and p35S:NRP-B-agroinoculated leaf sector. The extent of lipid peroxidation in leaf sectors agroinoculated with the indicated samples as in *A* was monitored by determining the MDA content. Values are given as mean ± S.D. from three replicates. *Asterisks* indicate values significantly different ($p < 0.05$, Student's *t* test). *D*, ethylene evolution in plants overexpressing *NRP-A* or *NRP-B*. Whole leaves of 3-week-old tobacco plants were agroinfiltrated with the indicated samples as in *A*; the plants were transferred to a sealed container, and ethylene evolution was monitored by gas chromatography. Values are given as mean ± S.D. from three replicates. *E*, induction of the senescence-associated gene *CP1* by *NRP-A* and *NRP-B* expression. Total RNA was isolated from agroinfiltrated leaf sectors, as indicated in *A*, and *CP1* induction was monitored by quantitative RT-PCR. Values are given as mean ± S.D. from three replicates.

expressing *NRP-B* or *NRP-A* (supplemental Fig. S5*B* and data not shown) displayed a chlorotic phenotype characteristic of leaf senescence that was associated with decreased chlorophyll content and consequent yellowing of the leaf sector (Fig. 4, *A* and *B*). This yellowing phenotype was attenuated by co-agroinfiltration of *NRP-A* or *NRP-B* with the senescence inhibitor, zeatin. The chlorophyll content of NRP-A and NRP-B-agroinoculated leaf sectors was significantly lower than that of the NIG-agroinoculated leaf sector control (Fig. 4*B*). Although inclusion of zeatin did not appear to revert NRP-A- and NRP-B-induced chlorophyll loss as indicated by Student's *t* test analysis ($p > 0.05$), it kept a similar level of chlorophyll in the leaf sectors agroinoculated with control and test genes.

We further examined the *NRP-A*- and *NRP-B*-induced senescence phenotype by measuring the accumulation of malondialdehyde (MDA), a major product of lipid peroxidation that, along with generation of active oxygen species, is associated with chlorophyll loss (35). A significant enhanced accumulation of reactive aldehydes derived from lipid peroxidation was observed in either *NRP-A*- or *NRP-B*-agroinoculated leaf slices in comparison with control samples and zeatin-pretreated *NRP-A*- or *NRP-B*-agroinoculated samples (Fig. 4*C*). Leaf yellowing and enhanced accumulation of MDA were a direct result of *NRP-A* or *NRP-B* expression and not a result of agrobacterium interactions, because expression of an unrelated, control protein (NIG, supplemental Fig. S5) did not cause yellowing of the agroinoculated sectors (Fig. 4*A*), and MDA synthesis (Fig. 4*C*) in the NIG-agroinoculated leaf sector was similar to that in leaf sectors where senescence was inhibited by zeatin.

The response to zeatin and loss of chlorophyll along with an increase in lipid peroxidation suggest the possibility that NRP-A and NRP-B trigger a response similar to senescence, a form of programmed cell death (36, 37). To further examine this possibility, we measure the evolution of ethylene synthesis, a well-known senescence hormone, and induction of known

Downloaded from http://www.jbc.org/ at CAPES - EMBRAPA on May 21, 2018

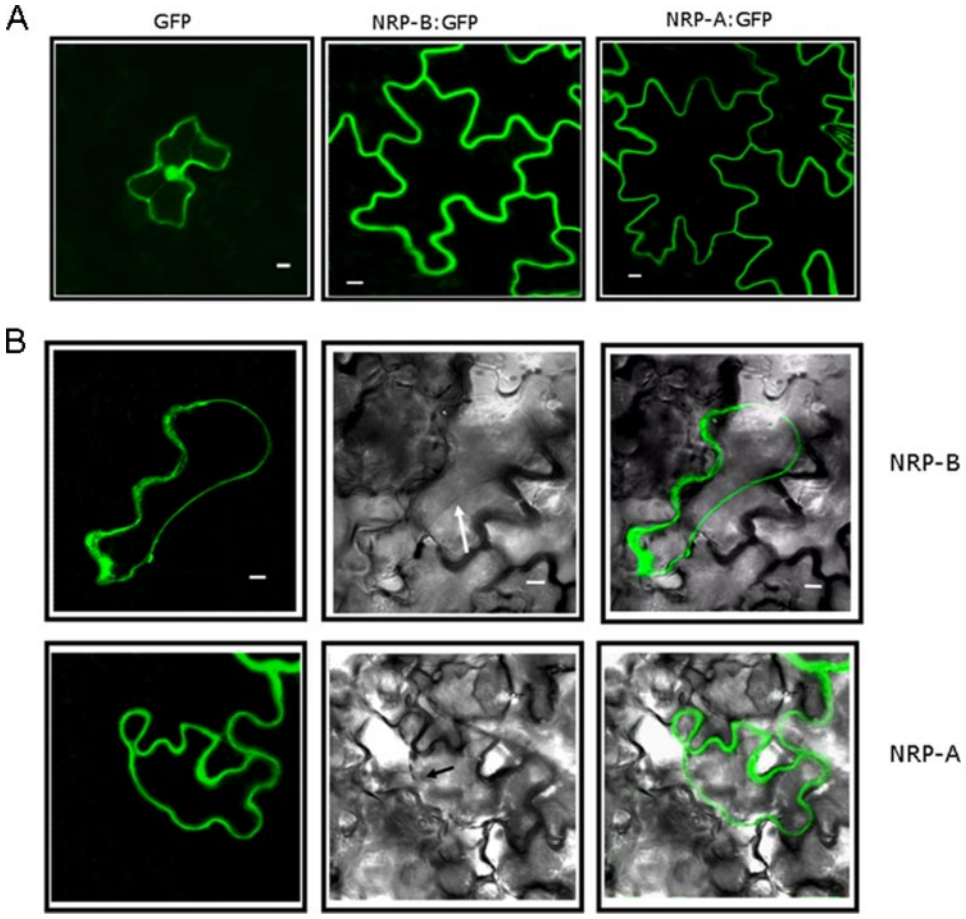

FIGURE 5. **Confocal microscopy analyses of NRP-A and NRP-B fused to GFP.** *A*, subcellular localization of 35S:GFP, NRP-A, and NRP-B fused to GFP. Tobacco leaves were infiltrated with *A. tumefaciens* carrying the indicated DNA construct, and images were taken by confocal laser scanning microscopy 72-h post-transfection. *Scale bars* are 10 μm. *B*, plasma membrane retention of confocal fluorescence after plasmolysis of NRP-A-GFP- and NRP-B-GFP-infiltrated leaves. Three days post-infiltration with p35S:NRP-A or p35S:NRP-B agroinoculum, excised leaf segments were treated with 0.6 M mannitol prior to microscopy. The *arrow* in the bright field shows a plasma membrane section detached from the cell wall. The superimposition of images confirms that the fluorescent recombinant protein remained with the detached plasma membrane.

senescence-associated genes. For ethylene measurement, the entire leaves from young tobacco plants were individually agroinoculated with *NRP-A*- or *NRP-B*-derived binary vectors and transferred to a sealed container. One week post-agroinfiltration, the ethylene content was measured by gas chromatography (Fig. 4*D*). Ethylene production was higher in *NRP-A*- and *NRP-B*-agroinoculated plants than in control plants agroinfiltrated with the unrelated gene *NIG*. Inclusion of the senescence inhibitor zeatin in the agroinoculum prevented NRP-A- or NRP-B-induced ethylene evolution in agroinfiltrated leaves.

In addition to the physiological responses related to senescence, we assayed expression of the senescence-associated gene marker, *CP1* (cysteine protease 1), by quantitative RT-PCR (Fig. 4*E*). *NRP-A* and *NRP-B* induced the expression of *CP1* when transiently expressed in tobacco leaves. This effect was antagonized by pretreatment of the leaves with the senescence inhibitor zeatin. Collectively, these results substantiate the argument that both NR proteins are functionally involved in programmed cell death processes.

Subcellular Localization of NRP-A and NRP-B Fused to GFP—The deduced NRP-A and NRP-B proteins do not contain any predicted signal of subcellular localization, although NRP-A was detected in a cell wall fraction of soybean cells undergoing a hypersensitive response (27). We investigated the localization of NRP-A and NRP-B, to see if it might provide additional clues to the function of these proteins in the integrated pathway. We utilized an *Agrobacterium*-mediated transient expression assay in epidermal cells of tobacco leaves and imaged NRP-A and NRP-B fused to GFP by confocal microscopy (Fig. 5). Both NRP-A and NRP-B fusions were targetted to the cell surface (Fig. 5*A*). We induced plasmolysis by treatment of the leaf sectors with 0.6 M mannitol to promote detachment of the plasma membrane from the cell wall. Both NRP-A-GFP and NRP-B-GFP remained in the area lining the detached plasma membrane leaving a fluorescent-free cell wall (Fig. 5*B*). These results rule out a cell wall location for the GFP-fused proteins when transiently expressed under control of the 35S promoter. However, because of the large central vacuole of leaf epidermal cells, the cytoplasm is pressed against the plasma membrane and hence appears in confocal slices as a narrow band. Therefore, it is not clear whether the observed fluorescence is derived from the plasma membrane, tonoplast, cytosol, or other organelles. Because the fused proteins were detected in microsomal fractions prepared from tobacco leaves transiently expressing NRP-A-GFP or NRP-B-GFP (data not shown), NRPs may be associated with membranes.

We also monitored the functional performance of GFP-fused proteins *in planta* as means to certify that fusion of GFP to the NRP-A and NRP-B C termini would not have caused mislocalization of the protein. Transient expression of [35S]NRP-A-GFP or [35S]NRP-B-GFP induced yellowing of leaves and chlorophyll loss one-week post-agroinoculation (supplemental Fig. S6) and confirmed that the GFP-fused proteins were functional. These results suggest that the localization of the fused proteins may reflect that of the intact proteins as well.

DISCUSSION

Previously we performed a global expression profiling on soybean leaves exposed to PEG treatment (osmotic stress) or to ER stress inducers and identified integrated networks between osmotic and ER stress-induced adaptive responses (4). A combination of the ER stress- and osmotic stress-induced treatments promoted a synergistic effect on the induction level of common up-regulated genes, indicating that the ER stress

Downloaded from http://www.jbc.org/ at CAPES - EMBRAPA on May 21, 2018

response integrates the osmotic signal to potentiate transcription of shared target genes. Among them, N-richI and N-richII ESTs showed the strongest synergistic induction by ER and osmotic stress. Upon further investigation, we found that the N-richI and N-richII ESTs represent the same gene, named *NRP-B*, which shares a high degree of identity with a previously identified N-rich protein (NRP) gene that we designate *NRP-A*. Like *NRP-B*, *NRP-A* may be considered to be a target of the integrated pathway, as it is synergistically and rapidly up-regulated by simultaneous induction of ER and osmotic stress. Three lines of evidence indicated that NRP-A and NRP-B mediate an apoptosis-like response in plants presumably through their DCD domains. Firstly, both genes were induced by cycloheximide, an apoptosis inducer, but repressed by the senescence inhibitors BAP and zeatin. Secondly, expression of *NRP-A* and *NRP-B* in soybean protoplasts induced caspase-3-like activity and DNA fragmentation. Finally, transient expression of *NRP-A* and *NRP-B in planta* accelerated senescence, as determined by the rapid development of leaf yellowing, that was accompanied by decreased chlorophyll content, increased MDA production, increased ethylene evolution, and induction of the senescence-associated gene marker *CP1*. The senescence inhibitor zeatin markedly prevented the development of NRP-A- and NRP-B-induced symptoms. Supplementation of the *NRP-A* or *NRP-B* agroinoculum with zeatin reduced leaf yellowing, chlorophyll loss, and MDA synthesis as well as prevented ethylene evolution and induction of senescence-associated gene markers. These results further substantiated the argument that *NRP-A* and *NRP-B* promote programmed cell death and leaf senescence.

Our results clearly indicated that ER and osmotic stress converge upon *NRP-A* and *NRP-B* to potentiate a senescence-like response. The induction of leaf senescence by drought stress, which shares signaling components with osmotic stress, is a well-documented phenomenon in plants (38). However, a direct link between prolonged ER stress and leaf senescence has not been previously demonstrated, although recent studies have shown that, like in mammalian cells, ER stress induces cell death and apoptotic-like responses in plants as well (33, 39–42). The recent work by Watanabe and Lam (42) further demonstrated that inactivation of the *Arabidopsis* BAX (BCL2-associated X protein) inhibitor 1 (*AtBI1*) accelerated the ER stress-induced PCD progression in roots. They proposed that *AtBI1* modulates a PCD execution program upon ER stress signaling. Although the mechanisms by which ER stress triggers specific programs of cell death in plants remains unknown, indirect evidence indicates that ER stress-induced PCD may occur through the molecular chaperone-inducing branch of UPR as well as by a distinct signal transduction cascade (43). This hypothesis is based on studies with ER stress inducers that identified *AtBI1* and the PCD-related *Hsr203J,* as UPR genes (5, 44). The presence of an ERSE-like cis-acting regulatory element in the *AtBI1* promoter suggested that up-regulation of the *BI* gene by ER stress may occur through the molecular chaperone-inducing branch of plant UPR (5). This hypothesis was strengthened by the recent demonstration that accumulation of unfolded protein in the ER controls the *AtBI1* promoter activity (42). In contrast, the delayed kinetics of *Hsr203J* induction in comparison with that of the UPR-specific target *BiP* and *PDI* genes indicated that ER stress may induce the PCD-related *Hsr203J* gene through a pathway independent from UPR (44). Here we showed that ER stress induces leaf senescence by activating plant-specific *NRPs* through a pathway distinct from the ER stress-specific branches of UPR. This interpretation is supported by several lines of evidence. First, activation of the NRP-mediated senescence-like response is not specific to ER stress but rather is a shared branch of general environmental adaptive pathways. In fact, *NRPs* are also induced by other abiotic and biotic signals, such as osmotic stress, drought, and pathogen incompatible interactions (27). Secondly, the molecular chaperone-inducing branch of UPR is inversely regulated by osmotic stress, whereas full induction of *NRPs* is dependent on both ER and osmotic stress signals (Fig. 1*B*). Finally, while induction of UPR-specific target genes, such as *BiP* and *CNX*, is prevented in soybean transgenic lines defective for UPR activation, *NRP-A* and *NRP-B* expression is up-regulated to a similar extent as in wild-type plants.

Recently, the subunit Gβ of the heterotrimeric G protein has been demonstrated to associate partially with ER membranes and to be involved in the signaling events that trigger UPR-associated cell death in plants (41). Inactivation of the Gβ gene in *Arabidopsis* impairs tunicamycin-induced cell death and attenuates the ER stress-induced transcriptional response of UPR-specific target genes, such as *BiP* and *PDI*, in Gβ-null alleles. Because Gβ signaling seems to be coupled (at least partially) to the molecular chaperone-inducing branch of UPR, it is unlikely that induction of *NRPs* by ER stress may be connected to the cell death-inducing Gβ signaling. More likely, ER stress-induced leaf senescence through activation of *NRP* expression describes a novel branch of the ER stress response in plants that shares components with the osmotic stress signaling.

In mammalian cells, ER stress has been shown to trigger both ER stress-specific apoptotic pathways and shared PCD signaling pathways elicited by other death stimuli (11). The NRP-mediated PCD signaling fits the concept of a shared pathway induced by ER stress and other stimuli, which is consistent with the localization of NRPs either as cytosolic or membrane-associated proteins. The lack of canonical transmembrane domains in the NRP-deduced primary structure suggests that any possible interaction of NRPs with plasma membrane would be either mediated by post-translational modification or by association with transmembrane proteins. Several cell surface death receptors have been identified in mammalian cells as the mediators of the cell death-inducing extrinsic pathway (45). Upon activation by ligand binding, the cytoplasmic domain of these death receptors recruits adaptor proteins to activate caspase cascades that result in morphological changes associated with apoptosis (32). The cytosolic or membrane-associated localization of NRPs, their rapid response to programmed cell death inducers along with their capacity to induce caspase-3-like activities in soybean protoplasts are consistent with a model in which NRPs would act as adaptor proteins that activate upstream initiator caspases. The identification of downstream targets and induction regulators of NRPs is crucial to elucidate the underlying mechanism of this ER- and osmotic stress-induced cell death

Downloaded from http://www.jbc.org/ at CAPES - EMBRAPA on May 21, 2018

signaling that transduces a PCD signal into multiple hallmarks of leaf senescence.

Acknowledgments—We thank the UFV microscopy core facility for the use of the LSCM and Prof. Chris Hawes for the ^{35}S-YFP-cassetteA-Nos-pCAMBIA1300 binary vector.

REFERENCES

1. Maa, Y., and Hendershot, L. M. (2004) *J. Chem. Neuroanatomy* **28,** 51–65
2. Buzeli, R. A. A., Cascardo, J. C. M., Rodrigues, L. A. Z., Andrade, M. O., Loureiro, M. E., Otoni, W. C., and Fontes, E. P. B. (2002) *Plant Mol. Biol.* **50,** 757–771
3. Denecke, J., Carlsson, L. E., Vidal, S., Hoglund, A.-S., Ek, B., van Zeiji, M. J., Sinjorgo, K. M. C., and Palva, E. T. (1995) *Plant Cell* **7,** 391–406
4. Irsigler, A. S., Costa, M. D., Zhang, P., Reis, P. A. B., Dewey, R. E., Boston, R. S., and Fontes, E. P. B. (2007) *BMC Genomics* **8,** 431
5. Kamauchi, S., Nakatani, H., Nakano, C., and Urade, R. (2005) *Febs. J.* **272,** 3461–3476
6. Kirst, M. E., Meyer, D. J., Gibbon, B. C., Jung, R., and Boston, R. S. (2005) *Plant Physiol.* **138,** 218–231
7. Martinez, I. M., and Chrispeels, M. J. (2003) *Plant Cell* **15,** 561–576
8. Koizumi, N., Martinez, I. M., Kimata, Y., Kohno, K., Sano, H., and Chrispeels, M. J. (2001) *Plant Physiol.* **127,** 949–962
9. Iwata, Y., and Koizumi, N. (2005) *Proc. Natl. Acad. Sci. U. S. A.* **102,** 5280–5285
10. Liu, J.-X., Srivastava, R., Che, P., and Howell, S. H. (2007) *Plant Cell* **19,** 4111–4119
11. Malhotra, J. D., and Kaufman, R. J. (2007) *Semin. Cell Dev. Biol.* **18,** 716–731
12. Leborgne-Castel, N., Jelitto-Van Dooren, E., Crofts, A. J., and Denecke, J. (1999) *Plant Cell* **11,** 459–469
13. Alvim, F. C., Carolino, S. M. B., Cascardo, J. C. M., Nunes, C. C., Martinez, C. A, Otoni, W. C., and Fontes, E. P. B. (2001) *Plant Physiol.* **126,** 1042–1054
14. Denekamp, M., and Smeekens, S. C. (2003) *Plant Physiol.* **132,** 1415–1423
15. Kreps, J. A., Wu, Y. J., Chang, H. S., Zhu, T., Wang, X., and Harper, J. F. (2002) *Plant Physiol.* **130,** 2129–2141
16. Seki, M., Narusaka, M., Ishida, J., Nanjo, T., Fujita, M., Oono, Y., Kamiya, A., Nakajima, M., Enju, A., Sakurai, T., Satou, M., Akiyama, K., Taji, T., Yamaguchi-Shinozaki, K., Carninci, P., Kawai, J., Hayashizaki, Y., and Shinozaki, K. (2002) *Plant J.* **31,** 279–292
17. Cascardo, J. C. M., Almeida, R. S., Buzeli, R. A. A., Carolino, S. M. B., Otoni, W. C., and Fontes, E. P. B. (2000) *J. Biol. Chem.* **275,** 14494–14500
18. Fontes, E. P. B., Eagle, P. A., Sipe, P. S., Luckow, V. A., and Hanley-Bowdoin, L. (1994) *J. Biol. Chem.* **269,** 8459–8465
19. Carvalho, C. M., Fontenelle, M. R., Florentino, L. H., Santos, A. A., Zerbini, F. M., and Fontes, E. P. B. (2008) *Plant J.*, in press
20. Aragão, F. J. L., Sarokin, L., Vianna, G. R., and Rech, E. L. (2000) *Theor. Appl. Genet.* **101,** 1–6
21. Pagny, S., Cabanes-Macheteau, M., Gillikin, J., Leborgne-Castel, N., Lerouge, P., Boston, R. S., Faye, L., and Gomord, V. (2000) *Plant Cell* **12,** 739–755
22. Delú-Filho, N., Pirovani, C. P., Pedra, J. H. F., Matrangolo, F. S. V., Macêdo, J. N. A., Otoni, W. C., and Fontes, E. P. B. (2000) *Plant Physiol. Biochem.* **38,** 353–353
23. Batoko, H., Zheng, H. Q., Hawes, C., and Moore, I. (2000) *Plant Cell* **12,** 2201–2218
24. Pirovani, C. P., Macêdo, J. N. A., Contim, L. A. S., Matrangolo, F. S. V., Loureiro, M. E., and Fontes, E. P. B. (2002) *Eur. J. Biochem.* **269,** 3998–4008
25. Lichtenthaler, H. K. (1987) *Methods Enzymol.* **148,** 350–382
26. Cakmak, I., and Horst, W. J. (1991) *Physiol. Plantarum* **83,** 463–468
27. Ludwig, A. A., and Tenhaken, R. (2001) *Eur. J. Plant Pathol.* **107,** 323–336
28. Tenhaken, R., Doerks, T., and Bork, P. (2005) *BMC Bioinformatics* **6,** 169
29. Cascardo, J. C. M., Buzeli, R. A. A., Almeida, R. S., Otoni, W. C., and Fontes, E. P. B. (2001) *Plant Sci.* **160,** 273–281
30. Wertz, I. E., and Hanley, M. R. (1996) *Trend Biochem. Sci.* **21,** 359–364
31. Woltering, E. J., Bent, A. V. D., and Hoeberichts, F. A. (2002) *Plant Physiol.* **130,** 1764–1769
32. Earnshaw, W. C., Martins, L. M., and Kaufmann, S. H. (1999) *Annu. Rev. Biochem.* **68,** 383–424
33. Zuppini, A., Navazio, L., and Mariani, P. (2004) *J. Cell Sci.* **117,** 2591–2598
34. Singh, S., Letham, D. S., and Palni, L. M. S. (1992) *Physiol. Plant* **86,** 388–397
35. Dhindsa, R. S., Plumb-Dhindsa, P., and Thorpe, T. A. (1981) *J. Exp. Bot.* **32,** 93–101
36. Greenberg, J. T. (1996) *Proc. Natl. Acad. Sci. U. S. A.* **93,** 12094–12097
37. Quirino, B. F., Noh, Y. S., Himelblau, E., and Amasino, R. M. (2003) *Curr. Opin. Plant Biol.* **6,** 79–84
38. Gan, S., and Amasino, R. M. (1997) *Plant Physiol.* **113,** 313–319
39. Crosti, P., Malerba, M., and Bianchetti, R. (2001) *Protoplasma* **216,** 31–38
40. Malerba, M., Cerana, R., and Crosti, P. (2004) *Protoplasma* **224,** 61–70
41. Wang, S., Narendra, S., and Fedoroff, N. (2007) *Proc. Natl. Acad. Sci. U. S. A.* **104,** 3817–3822
42. Watanabe, N., and Lamb, E. (2008) *J. Biol. Chem.* **283,** 3200–3210
43. Urade, R. (2007) *FEBS J.* **274,** 1151–1171
44. Iwata, Y., and Koizumi, N. (2005) *Planta* **220,** 804–807
45. Ashkenazi, A., and Dixit, V. M. (1998) *Science* **281,** 1305–1308

Downloaded from http://www.jbc.org/ at CAPES - EMBRAPA on May 21, 2018

A New Branch of Endoplasmic Reticulum Stress Signaling and the Osmotic Signal Converge on Plant-specific Asparagine-rich Proteins to Promote Cell Death

Maximiller D. L. Costa, Pedro A. B. Reis, Maria Anete S. Valente, André S. T. Irsigler, Claudine M. Carvalho, Marcelo E. Loureiro, Francisco J. L. Aragão, Rebecca S. Boston, Luciano G. Fietto and Elizabeth P. B. Fontes

J. Biol. Chem. 2008, 283:20209-20219.
doi: 10.1074/jbc.M802654200 originally published online May 19, 2008

Access the most updated version of this article at doi: 10.1074/jbc.M802654200

Alerts:
- When this article is cited
- When a correction for this article is posted

Click here to choose from all of JBC's e-mail alerts

Supplemental material:
http://www.jbc.org/content/suppl/2008/05/20/M802654200.DC1

This article cites 44 references, 20 of which can be accessed free at
http://www.jbc.org/content/283/29/20209.full.html#ref-list-1

Downloaded from http://www.jbc.org/ at CAPES - EMBRAPA on May 21, 2018